## Aethalometer® - AE36s

**Expand the frontiers of aerosol science with cutting-edge Black Carbon instrument** 

White paper



Ljubljana, February 2024

Contents

#### Aethalometer® - AE36s

1.	Summary	3
2.	DualSpot™ technology	5
3.	Source Apportionment	8
4.	Real-time determination of Brown Carbon	10
	Advanced characterization of light-absorbing organic aerosoletion (9-λ)	13
	Advanced apportionment of Carbonaceous Aerosol (connectivity A08)	
7.	Relative humidity robustness	19
8.	AE36s performance	22

New GUI design ...... 23

12. Automatic Zero and Span2713. Remote Access System (RAS)2914. User and Communications Interfaces3015. Modular Construction3016. Contact31

## 1. Summary

The Aethalometer is the most widely used filter photometer capable of measuring the light-absorbing properties of aerosol particles. Its robust design, ease of use, and quality data allow it to be used in different environments and numerous applications. The new AE36s is built upon the existing well-proven and rugged design. Two new wavelengths, 340 and 400 nm, were added for advanced characterization of light-absorbing organic aerosol fraction, the so-called Brown Carbon (BrC). We improved the performance of the Aethalometer, making it insensitive to RH changes. lowering the LOD, and making the operation of the Instrument even smoother with the new point-of-load electronics design. It is made to run unattended for a very long time thanks to the new self-cleaning procedure, 2-times longer filter tape, and the new RAS (Remote Access System) module in the updated CAAT software for a seamless network connection wherever you are. To add ease of use, we redesigned the graphical user interface, including real-time data visualization, providing a quick check of the data on-site. Data handling is now faster with automatic data validation. The AE36s is thus the first Instrument in the world that helps authorities to follow WHO 2021 recommendations in developing standards or targets for ambient Black Carbon (BC) concentrations.

The most important new features of the AE36s are:

- Advanced characterization of aerosol sources and aging state using 9wavelengths, 340 – 950 nm,
- Real-time Brown Carbon analyses using two new wavelengths, 340 and 400 nm.
- New filter compartment design <u>eliminates the instruments' sensitivity to</u> the changes in relative humidity (RH).
- Graphical presentation of data in time series or wind-rose.
- Simplified maintenance with the self-cleaning procedure (SCP).
- Automatic data validation with new status control.
- Straightforward network connection for remote management and data transfer with Remote Access Software (RAS).
- Hermetic seals prevent the ingress of dust and moisture.

The AE36s keeps the most important features of its predecessor:

- Patented <u>'Dual Spot' technology</u> eliminates the data artifact due to the filter loading effect.
- Integrates with TCA08 for OC/EC analysis.

#### AEROSOL MAGEE SCIENTIFIC

- Analysis at <u>multiple wavelengths</u> allows real-time Black Carbon source apportionment to fossil fuel and biomass burning.
- Automatic flow calibration procedure using external standards ensures accuracy.
- Built-in 'zero' test from internal clean-air source checks leakage and noise.
- 'Span' test of optical detectors using external standards validates performance.
- Front-panel USB ports provide local download without interruption of data.
- Low power consumption (30 W) permits off-grid use.
- Completely automatic operation upon power-up provides continuity.
- Direct coupling to CO<sub>2</sub> sensor (optional accessory) integrates BC and CO<sub>2</sub> data.
- Direct coupling to meteorology sensor (optional accessory) reports P, T, and RH permits calculation of BC concentration data under 'local' conditions.
- AE36s data can be transferred to the Carbonaceous Aerosol Analysis Tool (CAAT), a desktop software for advanced analysis (averaging, diurnal profiles, calculating BrC, etc.).

## 2. DualSpot™ technology

The AE36s Aethalometer uses the patented Dual Sport™ method to compensate for the 'spot loading effect' and also to provide a real-time output of the 'loading compensation' parameter, which may provide additional information about the physical and chemical properties of the aerosol (Drinovec et al., 2015).

The 'spot loading effect' is a variable phenomenon that gradually reduces instrumental response as the aerosol deposit density of the filter tape increases from zero to the predetermined limit of 'Maximum Attenuation'. When the filter tape advances to a fresh spot, the data undergoes a discontinuous jump from its previous lower value, calculated when the spot was heavily loaded, to a higher value, calculated from collection on a fresh spot at zero loading. In the Aethalometer, the reduction of data at increasing loadings is well described by a linear function of attenuation, but its magnitude cannot be predicted: some aerosols in some locations in some seasons may show a small or zero 'loading effect', while under other conditions, the effect may be larger and noticeable. Empirically, it is found that fresher aerosols closer to their combustion sources will show a larger' spot loading effect'. In contrast, well-aged aerosols with high chemical activity and oxidative processing may show almost zero effect under atmospheric conditions. The effect is revealed statistically by processing data collected over many tape advances, representing many data points collected at loadings, i.e., attenuation (ATN) values ranging from zero to the preset maximum. The data is collected into bins according to loading. Suppose the calculated result is systematically reduced as a loading function. The data will show a clear negative slope, with the intercept representing the 'zero loading' value.

An instrument based on firmware with a fixed 'loading non-linearity' parameter will not operate correctly at all locations. The 'loading non-linearity' parameter must be measured.

Thus, the loading effect phenomenon can be represented as

BC (reported) = BC (zero loading) \* { 1 - 
$$k \cdot ATN$$
 },

where BC (zero loading) is the desired ambient BC value obtained without any loading effect, and k is the 'loading compensation parameter'.

The analysis of many datasets from various locations shows that this relationship is linear in all cases studied but with different values of k. It is, therefore, possible to eliminate the 'loading effect' of k by making two simultaneous identical measurements, BC1 and BC2, at different degrees of loading  $ATN_1$  and  $ATN_2$ .

$$BC_1 = BC * \{ 1 - k \cdot ATN_1 \}$$
  
 $BC_2 = BC * \{ 1 - k \cdot ATN_2 \}$ 

aerosolmageesci.com

From these two linear equations, we may calculate the 'loading compensation parameter' k and the desired value of BC compensated back to zero loading.

The AE36 Aethalometer analyzes the Black Carbon component of aerosols on two parallel spots drawn from the same input stream but collected at different accumulation rates, i.e., at different values of ATN. By combining the data according to the above equations, the AE36 yields the value of BC extrapolated back to 'zero loading' and real-time output of the 'loading compensation parameter' k, which provides insights into the aerosol nature and composition. This process is performed in real-time for all wavelengths: examining the k values as a function of wavelength provides further information about the aerosol composition. An example of the real-time loading compensation process is shown in Fig. 1 for extreme concentrations of black carbon.

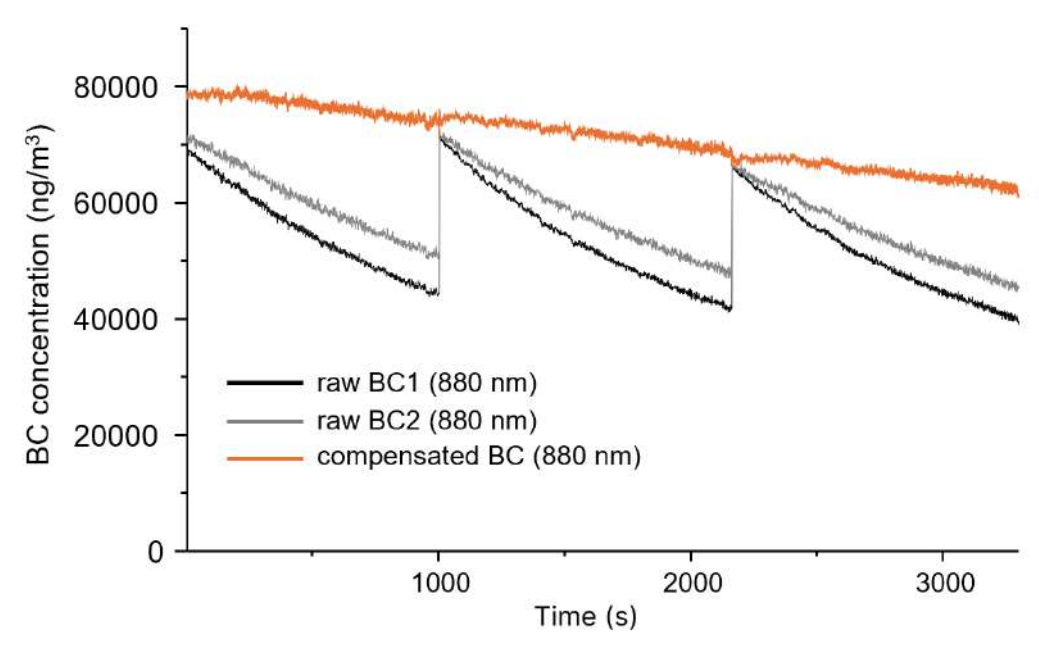


Figure 1. The time-series of Aethalometer raw and compensated BC concentrations with 1 second time base – note the extreme concentrations and loading effects.

Real-time loading compensation is essential for real-time source apportionment (see Chapter 3), as it is based on absorption data at 470 and 950 nm. Without loading compensation, the uncertainty in the source apportionment calculation increases significantly.

Other filter-based BC-measuring instruments also exhibit 'spot loading effects' (Kanaya et al., 2008; Virkkula, 2010; Hyvärinen et al., 2013). Published results show that the effect is not linear and consequently not readily amenable to mathematical compensation without making assumptions about the nature of the aerosol. However, with patented DualSpot™ technology, aerosol properties connected to the loading effect are not assumed but measured in real time.

#### AEROSOL MAGEE SCIENTIFIC

#### References:

Drinovec, L., Močnik, G., Zotter, P., Prévôt, A.S.H., Ruckstuhl, C., Coz, E., Rupakheti, M., Sciare, J., Müller, T., Wiedensohler, A., Hansen, A.D.A., 2015. The "dual-spot" Aethalometer: an improved measurement of aerosol black carbon with real-time loading compensation. Atmospheric Meas. Tech. 8, 1965–1979.

Virkkula A., 2010, Correction of the Calibration of the 3-wavelength Particle Soot Absorption Photometer (3λ PSAP), Aerosol Sci. Tech., 44, 706-712.

Hyvärinen et al., 2013, Correction for a measurement artifact of the Multi-Angle Absorption Photometer (MAAP) at high black carbon mass concentration levels, Atmos. Meas. Tech., 6, 81-90.

Kanaya et al., 2008, Mass concentrations of black carbon measured by four instruments in the middle of Central East China in June 2006, Atmos. Chem. Phys., 8, 7637–7649.

gerosolmageesci.com Page 7 of 31

## 3. Source Apportionment

Source apportionment of black carbon concentration is based on the Sandradewi et al. (2008) model, also called the "Aethalometer model", with the optical absorption coefficient being a sum of biomass burning and fossil fuel burning fractions. Some measurement networks are also introducing new terminology guidelines for the two fractions of black carbon, i.e., solid fuel and liquid fuel fractions. The model is based on the difference in absorption coefficient wavelength dependency, assuming that absorption due to fossil fuel and biomass emissions follow  $\lambda^{-\alpha_{ff}}$  and  $\lambda^{-\alpha_{bb}}$  spectral dependencies, respectively. The exponents describing the spectral dependence are absorption Ångström exponents (AAE). Default values used in the Aethalometer are  $\alpha_{ff}=1$  for fossil fuel and  $\alpha_{bb}=2$  for biomass. The following equations can be used to describe the absorption coefficient from both sources based on 470 nm and 950 nm absorption measurements:

$$\frac{b_{abs}(470 nm)_{ff}}{b_{abs}(950 nm)_{ff}} = \left(\frac{470}{950}\right)^{-\alpha_{ff}}$$
$$\frac{b_{abs}(470 nm)_{bb}}{b_{abs}(950 nm)_{bb}} = \left(\frac{470}{950}\right)^{-\alpha_{bb}}$$

$$b_{abs}(470 nm) = b_{abs}(470 nm)_{ff} + b_{abs}(470 nm)_{bb}$$
  
$$b_{abs}(950 nm) = b_{abs}(950 nm)_{ff} + b_{abs}(950 nm)_{bb}$$

where  $b_{abs}(\lambda)$  is the absorption coefficient at a specified wavelength,  $\lambda$  is the wavelength,  $b_{abs}(\lambda)_{ff}$  is a fossil fuel fraction and  $b_{abs}(\lambda)_{bb}$  a biomass burning fraction of absorption coefficient. Fraction of biomass burning BB(%) of black carbon (BC880) is:

$$BB(\%) = \frac{b_{abs}(950 nm)_{bb}}{b_{abs}(950 nm)}$$

Biomass burning and traffic-related BC fractions are then calculated as:

$$BC_{bb} = BB/100 \times BC$$
  

$$BC_{ff} = (1 - BB/100) \times BC$$

An example of the result of such source apportionment measurements in the intensive Comparative Study of Black Carbon and Other Carbonaceous Aerosols in Four Southeast European (SEE) Hotspots is depicted in Figure 2.

Settings and presentation

display of BB % on the Home screen.

- The percentage of BC emitted by biomass burning sources is stored in the Data table, column name BB.
- The algorithm can be fine-tuned by changing the value of absorption Ångström exponents  $\alpha_{ff}$  and  $\alpha_{bb}$  on the 'Settings' | Advanced' screen (Aff and Abb settings)
- The calculated values are limited to the 0-100% range.

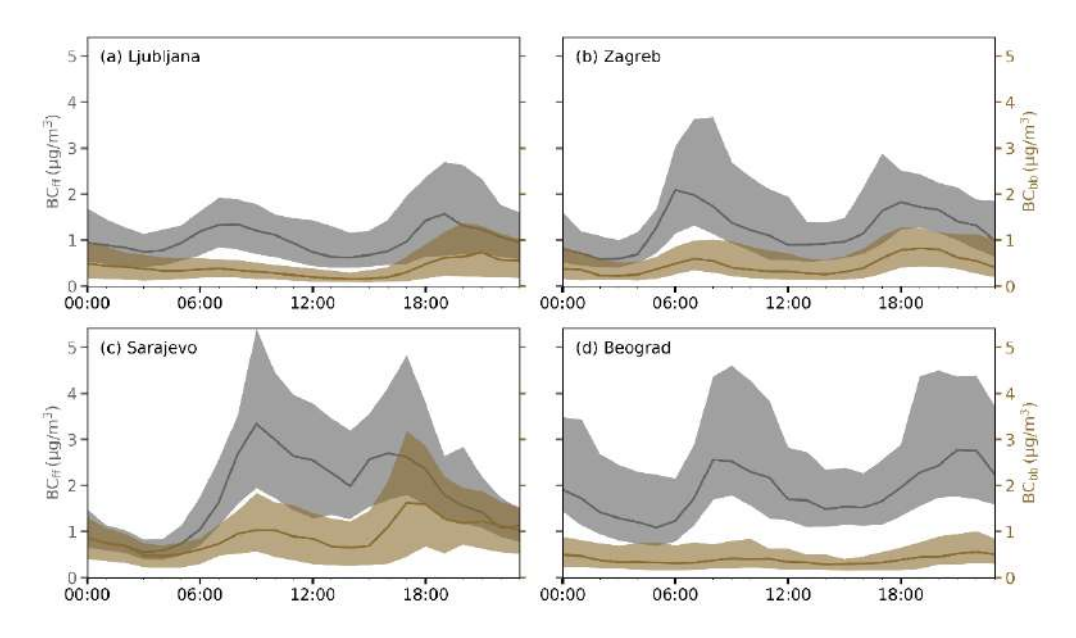


Figure 2 Display of diurnal profiles for BC<sub>ff</sub> and BC<sub>bb</sub> for four capital cities in the SEE region: (a) Ljubljana (Slovenia), (b) Zagreb (Croatia), Belgrade (Serbia), and Sarajevo (Bosnia and Herzegovina).

For real-time source apportionment, real-time filter loading compensation with a Dual Spot algorithm is needed. The source apportionment algorithm uses compensated data at wavelengths 950 and 470 nm. Using uncompensated measurements introduces significant uncertainty in the source apportionment calculation since it compares two measurements with different loading effects (loading effects vary with different wavelengths - different k values). Therefore, no filter photometer manufacturer, except AE36 and AE36s, can claim that their Instrument is capable of real-time source apportionment, as they do not have real-time filter loading compensation. The same applies to the real-time BrC model (see Chapter 4.).

#### Reference

Sandradewi, J. et al. (2008), Using Aerosol Light Absorption Measurements for the Quantitative Determination of Wood Burning and Traffic Emission Contributions to Particulate Matter, Environ. Sci. Technol. 42, 3316–3323.

gerosolmageesci.com Page 9 of 31

#### 4. Real-time determination of Brown Carbon

Organic aerosol (OA) can be divided into light-absorbing OA, also known as Brown Carbon (BrC) (Andreae & Gelencsér, 2006; Liu et al., 2020; Laskin et al., 2015), and non-light absorbing ('transparent') OA (OA<sub>non-abs</sub>). Both of these may have primary and secondary aerosol origins. BrC absorbs solar radiation mainly in the ultraviolet and short visible wavelength range.

BrC is a significant component of CA, and it arises from both primary combustion processes and secondary chemical reactions (Figure 3). It affects atmospheric visibility, Earth's radiation balance, and human health. The AE36s Aethalometer provides real-time BrC measurements with a high temporal resolution, which is important for the following aspects (Saleh et al., 2020):

- Climate Impact: BrC has a direct radiative effect, influencing the Earth's energy balance. Accurate, high-resolution measurements can help improve climate models and predictions.
- Health Effects: Some organic chromophores in BrC are extremely toxic, linking BrC to adverse health effects<sup>1</sup>. High-time resolution measurements can provide more detailed data on these harmful component<sup>1</sup>.
- Advanced Source Apportionment: High-resolution measurements can help identify the sources of BrC, such as biomass and biofuel combustion, lowefficiency coal combustion, and ship engines utilizing heavy fuel oil<sup>2</sup>.
- Atmospheric Aging: BrC undergoes changes in the atmosphere, including production of secondary BrC and the bleaching/darkening of primary BrC. Hightime resolution measurements can capture these dynamic processes.

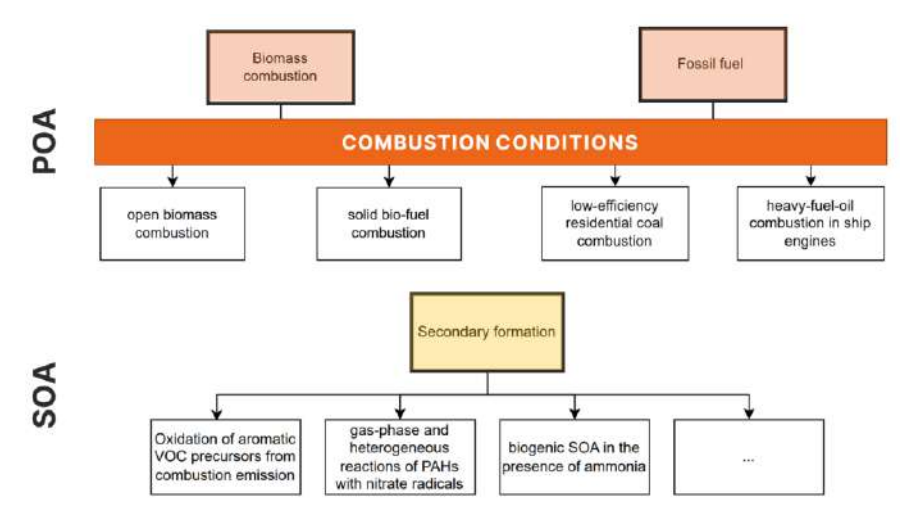


Figure 3. Brown carbon is emitted from both primary combustion processes and secondary chemical reactions.

The AE36s uses the following model for Brown Carbon. The wavelength-dependent optical absorption of carbonaceous aerosol can be apportioned into two components,  $b_{abs}^{BC}$  and  $b_{abs}^{BrC}$ :

$$b_{abs}(\lambda, t) = b_{abs}^{BC}(\lambda, t) + b_{abs}^{BrC}(\lambda, t),$$

where the wavelength dependence of each component can be described with  $AAE_{BC}$  and  $AAE_{BrC}(t)$ , the absorption Ångström exponent of pure BC and BrC, respectively:

$$\begin{split} b^{BC}_{abs}(\lambda,t) &= b^{BC}_{abs}(\lambda_0,t) \cdot \left(\frac{\lambda}{\lambda_0}\right)^{-AAE_{BC}}, \\ b^{BrC}_{abs}(\lambda,t) &= b^{BrC}_{abs}(\lambda_0,t) \cdot \left(\frac{\lambda}{\lambda_0}\right)^{-AAE_{BrC}(t)}. \end{split}$$

The BrC model in AE36s assumes that BC is the only absorber at 880 nm. The light absorption by BC for shorter wavelengths is then calculated with the extrapolation from 880 nm using a predefined Ångström exponent for BC ( $\alpha_{BC}$ ). The default value for this parameter in AE36s is 1.0 but can be changed by the user – 'Abc' setting on the 'Settings' | 'Advanced' screen. This type of BrC model offers a robust estimation of the light absorption coefficient on BrC. BrC absorption coefficient is calculated for each wavelength and reported in the Data table. Thus,

$$\begin{aligned} b_{abs}(880 \text{ nm, t}) &= b_{abs}^{BC}(880 \text{ nm, t}); \ b_{abs}^{BrC}(880 \text{ nm, t}) \ = 0 \\ b_{abs}^{BC}(\lambda, t) &= b_{abs}^{BC}(880 \text{ nm, t}) \cdot \left(\frac{\lambda}{880 \text{ nm}}\right)^{-AAE_{BC}} \end{aligned}$$

and finally, the wavelength-dependent optical absorption of BrC as

$$b_{abs}^{BrC}(\lambda,t) = b_{abs}(\lambda,t) \, - \, b_{abs}^{BC}(\lambda,t). \label{eq:babs}$$

Brown Carbon concentration is calculated from the BrC absorption coefficient at 400 nm by the following equation:

BrC = 
$$b_{abs}^{BrC}(\lambda, t)/MAC_{BrC(400)}$$

where MAC<sub>BrC(400)</sub> is the mass absorption coefficient for Brown Carbon (at 400 nm), the default value used in AE36s is 4.5 m²/g (Ivančič et al., 2022), but can be modified by the user on the 'Settings' | 'Advanced' screen, 'MAC BrC' setting. Since MAC<sub>BrC</sub> can vary as a function of organic carbon chemical composition, it is recommended that the most appropriate MAC<sub>BrC</sub> is selected based on available information from the scientific literature or defined from other available measurements.

AE36s Home Screen shows BrC information as BrC concentration (ng/m³) or a fraction of BrC absorption at 400 nm (Figure 4). This setting is set by the user in System/Display settings.

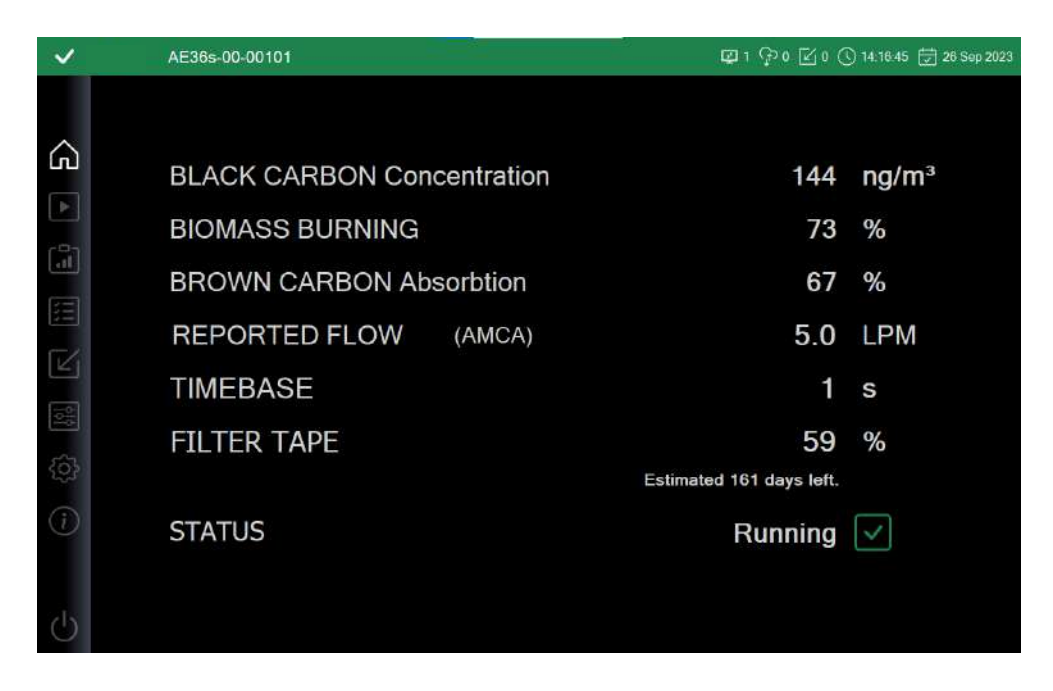


Figure 4. AE36s Home Screen shows BrC information as BrC concentration (ng/m3) or as a fraction of BrC absorption at 400 nm.

#### References

Andreae, M.O., Gelencsér, A., 2006. Black carbon or brown carbon? The nature of light-absorbing carbonaceous aerosols. Atmospheric Chem. Phys. 6, 3131–3148. <a href="https://doi.org/10.5194/acp-6-3131-2006">https://doi.org/10.5194/acp-6-3131-2006</a>

Liu, D., He, C., Schwarz, J.P., Wang, X., 2020. Lifecycle of light-absorbing carbonaceous aerosols in the atmosphere. Npj Clim. Atmospheric Sci. 3, 1–18. https://doi.org/10.1038/s41612-020-00145-8

Laskin, A., Laskin, J., Nizkorodov, S.A., 2015. Chemistry of Atmospheric Brown Carbon. Chem. Rev. 115, 4335–4382. https://doi.org/10.1021/cr5006167

Saleh, R., 2020. From Measurements to Models: Toward Accurate Representation of Brown Carbon in Climate Calculations. Curr. Pollut. Rep. 6, 90–104. https://doi.org/10.1007/s40726-020-00139-3

Ivančič M., Gregorič A., Lavrič G., Alföldy B., Ježek I., Hasheminassab S., Pakbin P., Ahangar F., Sowlat M., Boddeker S., et al. Two-Year-Long High-Time-Resolution Apportionment of Primary and Secondary Carbonaceous Aerosols in the Los Angeles Basin Using an Advanced Total Carbon–Black Carbon (TC-BC(λ)) Method. Sci. Total Environ. 2022;848:157606. doi: 10.1016/j.scitotenv.2022.157606.

gerosolmageesci.com Page 12 of 31

# 5. Advanced characterization of light-absorbing organic aerosol fraction $(9-\lambda)$

The quantification of aerosol light absorption is critical in assessing particulate matter's influence on radiative forcing and public health impact, especially carbonaceous aerosols.

Especially for BrC, it is crucial to investigate its optical properties at several wavelengths as there is a high variability of BrC chemical composition reflecting in unique spectral response and, during ageing, aerosol mixing state and changes in the chemical composition of BrC chromophores additionally influence absorption properties. BrC absorption and its optical properties based on the parametrization published by Saleh (2020) are schematically shown in Figure 5. The efficiency of light absorption by BrC is inversely correlated with the wavelength dependence of absorption. In simpler terms, larger chromophores (molecules responsible for color) tend to absorb light more effectively. These larger chromophores are less volatile and exhibit weak solubility. A strong correlation exists between the optical properties of BrC and the combustion conditions under which it is formed. BrC can be categorized into different types based on its absorption characteristics:

- Very weak absorbing BrC: It exhibits very weak BrC properties and has the highest angstrom exponent. The Angstrom exponent describes the spectral dependence of aerosol light absorption.
- Weak absorbing BrC: Primary BrC from smoldering is weakly absorbing. Similar properties are observed for secondary BrC originating from combustion sources.
- Medium absorbing BrC: In high-temperature combustion scenarios (e.g., residential biomass burning for heating), BrC is emitted alongside Black Carbon (BC). - BC and BrC are often found together in these conditions.
- <u>Strong absorbing BrC</u>: Another group of BrC chromophores exhibit strong absorption. - These chromophores are very stable at high temperatures, are insoluble, and are challenging to differentiate from black carbon. Examples include tar balls.

gerosolmageesci.com Page 13 of 31

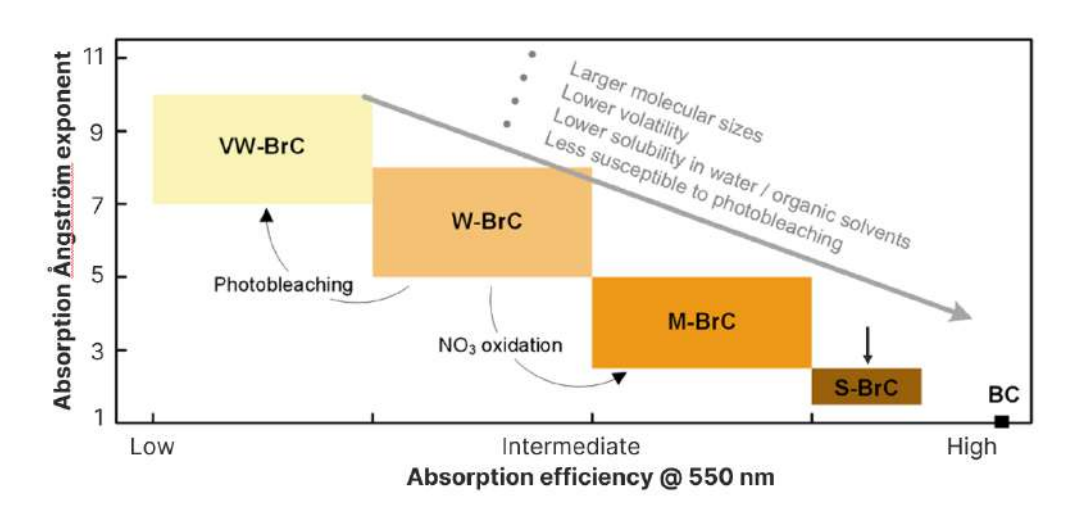


Figure 5. BrC can be categorized into different types based on its absorption efficiency and absorption Angstrom exponent.

The absorption Ångström exponent (AAE) can represent the spectral dependence of absorption, which is derived from a power law assumption. This metric is instrumental in characterizing light-absorbing aerosols, such as Black Carbon (BC) and Brown Carbon (BrC), and identifying their sources. The AAE is typically computed by applying a linear fit to the logarithmically transformed absorption measurements obtained at two or more wavelengths. However, it has been observed that absorption spectra display unique spectral characteristics across the ultraviolet and visible wavelength range. These features cannot be accounted for by extrapolation using a single power law function, indicating the need for more complex models or methods to describe the spectral behaviour of aerosol absorption accurately. This highlights the complexity of aerosol absorption properties and the necessity for advanced analytical techniques in aerosol optics research.

This is why introducing the two new wavelengths in AE36s in the UV and blue wavelength region: 340 and 400 nm (Figure 6). The additional number of wavelengths gives the possibility to develop a new approach to characterize the optical properties of aerosol light absorption using the AE36s Aethalometer, the so-called two-dimensional AAE (2D-AAE) approach (Gregorič et al., 2024)

aerosolmageesci.com Page 14 of 31

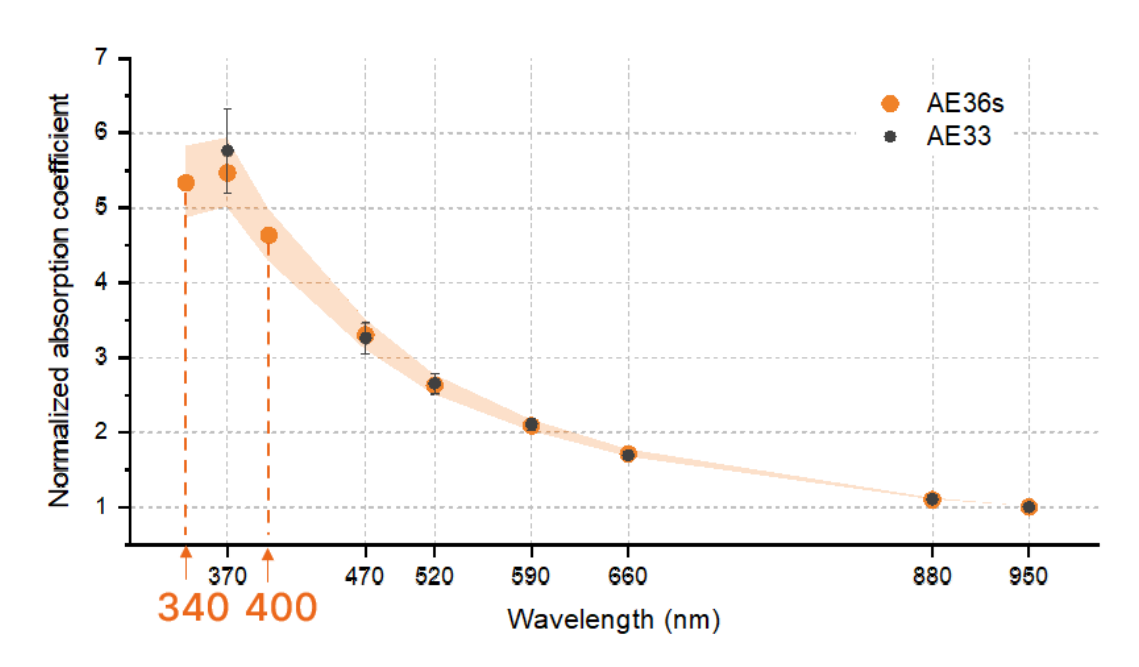


Figure 6. AE36s introduces two additional wavelengths in comparison to AE36 and AE33 in the UV and blue region for advanced BrC characterization.

The 2D-AAE approach uses two exponential functions to describe the optical properties of the aerosol light absorption, the shorter (AAE<sub>400-520nm</sub>) and longer (AAE<sub>590-950nm</sub>) wavelengths separately. The angstrom exponent in the shorter wavelengths is also used to extrapolate the absorption characteristics to the UV and observe the difference between measured and expected absorption at 340 nm. An example of two contrasting 2D-AAE measurements for fresh aerosols from a diesel engine (black) and the smouldering from burning wood (orange) is shown in Figure 7 together with the Helium lon Microscopy (HIM) images of the measured aerosols on the filter (Gregorič et al, 2024).

gerosolmageesci.com Page 15 of 31

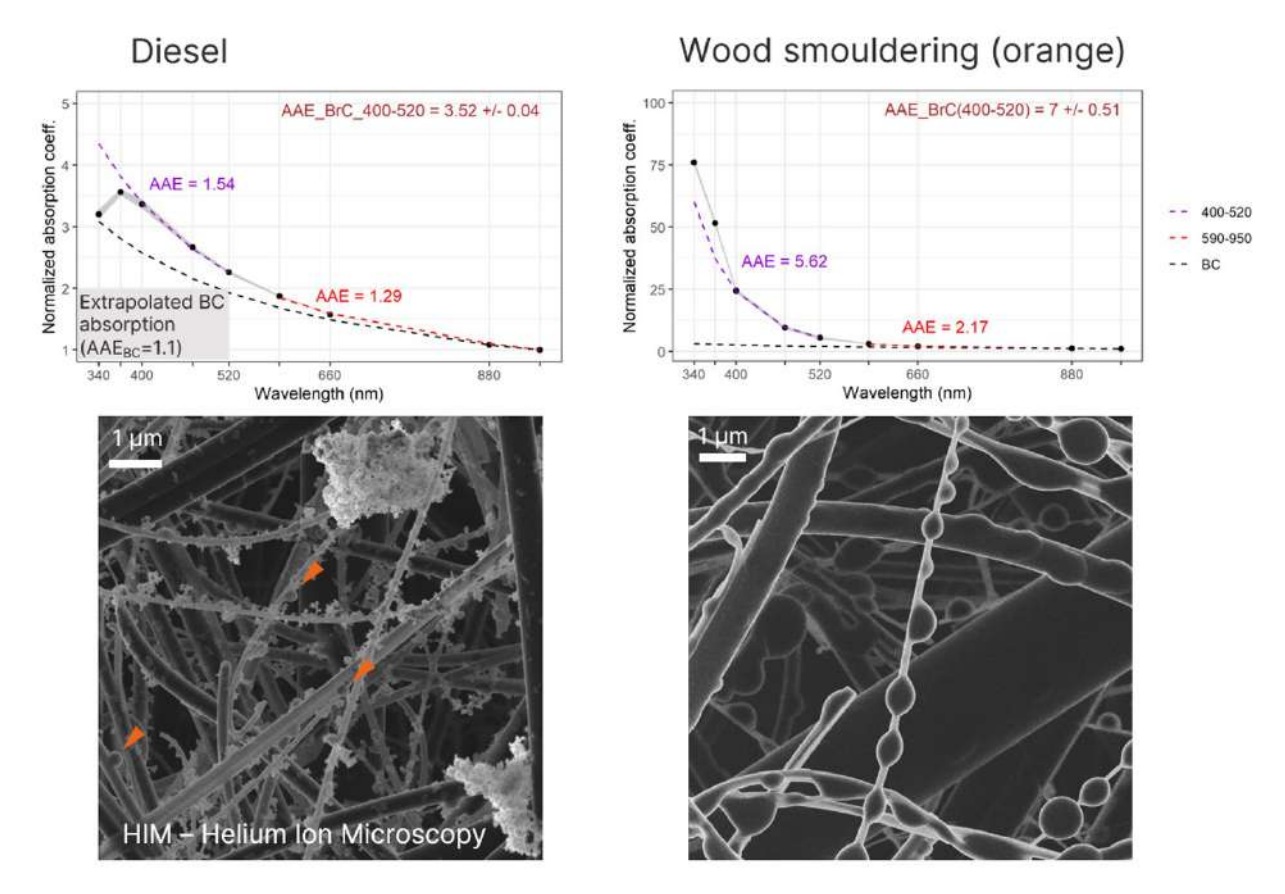


Figure 7. 2D-AAE measurements of fresh aerosols from a diesel engine and the smouldering from burning orange wood together with the Helium Ion Microscopy (HIM) images of aerosols on the filters.

#### References

Saleh, R., 2020. From Measurements to Models: Toward Accurate Representation of Brown Carbon in Climate Calculations. Curr. Pollut. Rep. 6, 90–104. https://doi.org/10.1007/s40726-020-00139-3

Gregorič. A., 2024. Advanced characterization of aerosol sources and aging state with the new 9λ Aethalometer model AE36s, *to be published*.

gerosolmageesci.com Page 16 of 31

# 6. Advanced apportionment of Carbonaceous Aerosol (connectivity to TCA08)

AE36s can be used in the CASS system (Carbonaceous Aerosol Speciation System; AE36 + TCA08) for the advanced TC-BC method (Rigler et al., 2020; Ivančič et al., 2022).

Carbonaceous aerosols (CA) represent extreme diversity and make up a large fraction of ambient fine particulate matter (PM<sub>2.5</sub>), acting as an atmospheric pollutant with critical local, regional, and global importance. The composition of CA provides a characteristic "fingerprint" and indicates the sources of airborne particulate matter.

Carbonaceous aerosol (CA) includes an organic fraction, organic aerosol (OA), and a refractory, strongly light-absorbing fraction referred to as black carbon (BC, optical measurement). The mass of carbon atoms in CA and OA is called total carbon (TC) and organic carbon (OC), respectively. The BC is chemically inert and has a well-defined chemical structure. It is exclusively emitted from incomplete combustion, thus having only a primary origin. OA is directly emitted to the atmosphere in particulate form as primary organic aerosols (POA) by combustion and from biogenic sources, or it can have a secondary origin, named secondary organic aerosols (SOA), formed by the oxidation of volatile organic compounds (VOC) in the atmosphere. Organic aerosol can be further divided into light-absorbing OA, also known as brown carbon (BrC) (Andreae and Gelencsér, 2006; Liu et al., 2020), and non-light-absorbing OA (OA<sub>non-abs</sub>), both with possible primary and secondary origin (POA<sub>BrC</sub>, SOA<sub>BrC</sub>, POA<sub>non-abs</sub>, SOA<sub>non-abs</sub>, respectively). While the OA<sub>non-abs</sub> have a cooling effect due to the scattering of the sunlight, BrC absorbs solar radiation mainly in the ultraviolet region (Laskin et al., 2015; Moise et al., 2015).

Apportionment of different components of carbonaceous aerosol relies on specific information available in the measured dataset. Simultaneous measurements of BC and TC result in a high-time-resolution organic carbon dataset. Spectrally resolved optical absorption measurements allow further differentiation to BrC and BC, which are closely linked to emission sources. Further information on the primary and secondary components takes advantage of highly time-resolved measurements, which provide important insight into the temporal behavior of different components. By applying different apportionment and numerical models from published studies, the CA was finally apportioned into six components (Figure 8):

$$\begin{aligned} \text{CA}(t) &= \text{BC}_{\text{ff}}(t) + \text{BC}_{\text{bb}}(t) + \text{POA}_{\text{non-abs}}(t) + \text{POA}_{\text{BrC}}(t) + \text{SOA}_{\text{non-abs}}(t) \\ &+ \text{SOA}_{\text{BrC}}(t) \end{aligned}$$

gerosolmageesci.com Page 17 of 31

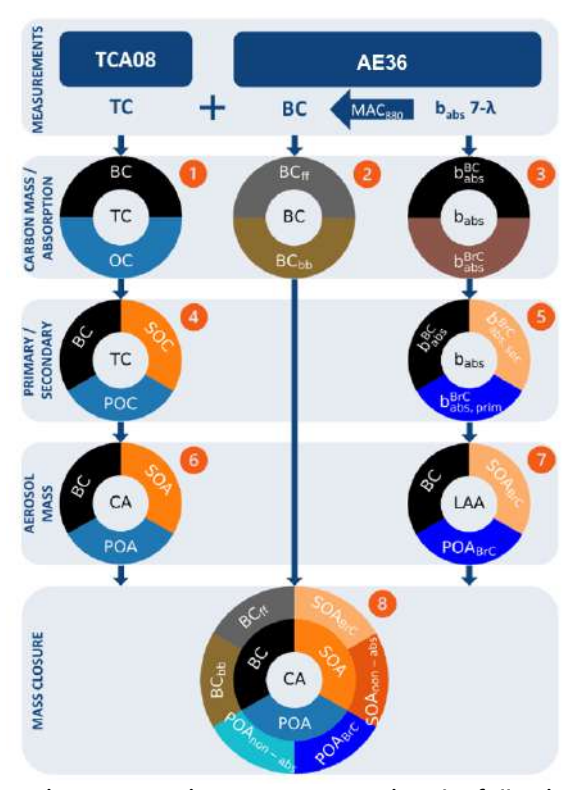


Figure 8: Flowchart for CA apportionment to six components using the following steps: 1. CASS measurements, 2. Aethalometer model, 3. BrC model, 4. BC tracer, 5. BC tracer for BrC, 6. Carbon content OA/OC, POA/POC, SOA/SOC, 7. Conversion of absorption to mass concentration using specific mass absorption cross-sections, 8. Non-light-absorbing OA determination.

#### **References**

Rigler, M., Drinovec, L., Lavrič, G., Vlachou, A., Prévôt, A.S.H., Jaffrezo, J.L., Stavroulas, I., Sciare, J., Burger, J., Kranjc, I., Turšič, J., Hansen, A.D.A., Močnik, G., 2020. The new Instrument using a TC–BC (total carbon–black carbon) method for the online measurement of carbonaceous aerosols. Atmospheric Meas. Tech. 13, 4333–4351. https://doi.org/10.5194/amt-13-4333-2020

Ivančič M., Gregorič A., Lavrič G., Alföldy B., Ježek I., Hasheminassab S., Pakbin P., Ahangar F., Sowlat M., Boddeker S., et al. Two-Year-Long High-Time-Resolution Apportionment of Primary and Secondary Carbonaceous Aerosols in the Los Angeles Basin Using an Advanced Total Carbon–Black Carbon (TC-BC(λ)) Method. Sci. Total Environ. 2022;848:157606. doi: 10.1016/j.scitotenv.2022.157606.

Laskin, A., Laskin, J., Nizkorodov, S.A., 2015. Chemistry of Atmospheric Brown Carbon. Chem. Rev. 115, 4335–4382. https://doi.org/10.1021/cr5006167

Moise, T., Flores, J.M., Rudich, Y., 2015. Optical Properties of Secondary Organic Aerosols and Their Changes by Chemical Processes. Chem. Rev. 115, 4400–4439. https://doi.org/10.1021/cr5005259

gerosolmageesci.com Page 18 of 31

## 7. Relative humidity robustness

Filter photometers are sensitive to changes in relative humidity (dRH/dt). Aerosol samples contain water vapor, which can be adsorbed to the fibers or to the binding material of the filter tape used in filter photometers, thus introducing noise in the data (Düsing et al., 2019). Water vapor can reach the filter through the sample inlet or enter through openings in the filter tape compartment, especially in environments where relative humidity changes rapidly (air-conditioned (AC) containers, mobile stations, etc.). The effects on BC measurements due to rapid changes in relative humidity as a result of AC operation in the vicinity of the predecessor of AE36s, Aethalometer AE33, are seen in Figure 9.

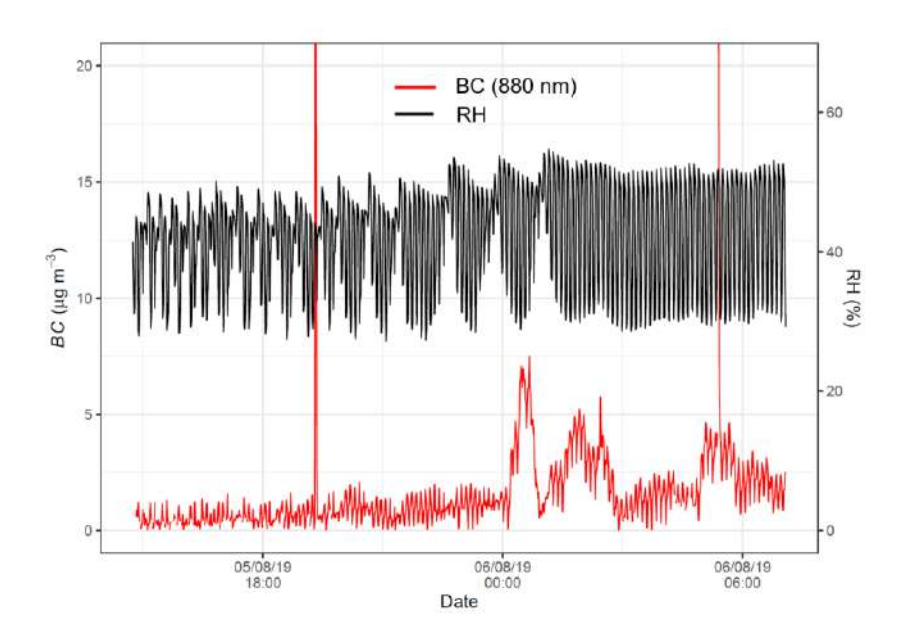


Figure 9 The effects on BC measurements due to rapid changes in relative humidity as a result of AC operation in the vicinity of the predecessor of AE36s, Aethalometer AE33

The changes of RH in the sample inlet can be reduced using Aerosol Inlet Dryer. The influence on the measurements due to rapid RH changes in the vicinity of the filter tape is reduced in the new Aethalometer AE36s with air sealing the filter tape compartment (Figure 10).

gerosolmageesci.com Page 19 of 31





Figure 10 Filter compartment of AE36s from the front and backside. Hermetic seals prevent dust and moisture ingress in the vicinity of filter tape.

In our simulation chamber, we replicated a situation where the humidity in the surroundings of the Instrument changed rapidly, simulating the fluctuation of RH introduced by AC. We controlled the temperature changes (T) and RH inside the simulation chamber while sampling clean air with stable RH. Our results showed that the AE36/AE36s were unaffected by the changes in RH (Figure ).

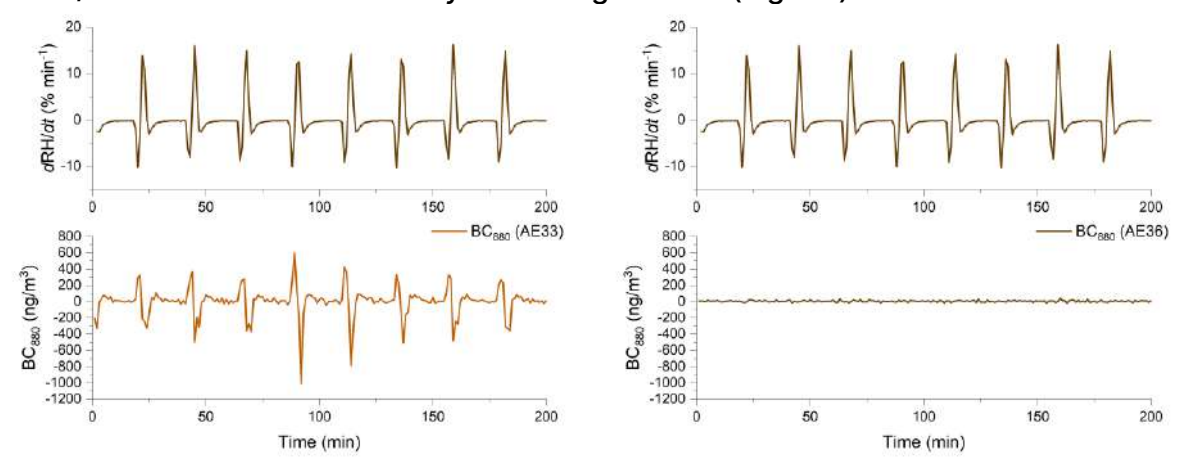


Figure 11. Simulation chamber with AE33(left) and AE36s (right) sampling clean air with stable RH. The humidity in the surroundings of the Instrument changed rapidly, simulating the fluctuation of RH introduced by AC. The AE36s was unaffected by the changes in RH.

To monitor the influence of RH and prevent damage caused by condensing water, we added two RH sensors in AE36s (Figure ). One is installed at the beginning of the inlet and monitors the humidity of the sampled air. If the air sample humidity exceeds the user-defined limit value, the Instrument will stop sampling and thus prevent water intrusion and probable damage to the flowmeters.

gerosolmageesci.com Page 20 of 31





Figure 12. Two RH sensors were installed in AE36s. The left position of the RH sensor is in the inlet line, and the right RH sensor is in the filter tape compartment.

The second sensor is installed in the filter chamber, monitoring changes of RH there-in. The Instrument will prompt a warning if the changes between two consecutive measurements are too high. Using both sensors, the user can meet the guidelines in the WMO/GAW Aerosol Measurement Procedures, Guidelines and Recommendations document.

#### References

GAW Report No. 227: WMO/GAW Aerosol Measurement Procedures, Guidelines and Recommendations, 2<sup>nd</sup> Edition, World Meteorological Organization, 2016

Düsing, S., Wehner, B., Müller, T., Stöcker, A., and Wiedensohler, A.: The effect of rapid relative humidity changes on fast filter-based aerosol-particle light-absorption measurements: uncertainties and correction schemes, Atmos. Meas. Tech., 12, 5879–5895, https://doi.org/10.5194/amt-12-5879-2019, 2019.

gerosolmageesci.com Page 21 of 31

## 8. AE36s performance

The AE36s enhanced performance characteristics, compared to its predecessor and other filter photometers on the market, are primarily attributed to several key technical improvements:

- 1. Relative Humidity (RH) Robustness: The influence on the measurements due to rapid RH changes in the vicinity of the filter tape is reduced in the new Aethalometer AE36s with air sealing the filter tape compartment.
- 2. Power Supply Design: The power supply circuitry has been significantly improved using the point of load design to provide stable and efficient power delivery, reducing the risk of performance degradation due to power fluctuations.
- 3. Firmware Signal Processing: Advanced signal processing algorithms implemented in the firmware enable more accurate and reliable data interpretation, contributing to the overall performance enhancement.
- 4. Air-Sealed Filter Compartment: The filter compartment is air-sealed, preventing the ingress of dust and other contaminants, thereby maintaining the integrity of the filter and the accuracy of measurements.

The table below provides a detailed specification of the AE36s key performance metrics, including Resolution, Limit of Detection (LoD), Precision, Measurement uncertainty, and measuring range. These metrics provide a comprehensive overview of the AE36s capabilities and performance characteristics. Please note that these values are subject to change based on operating conditions and calibration.

Parameter	AE33	AE43	AE36s
Resolution	$<1 \text{ ng/m}^3 @ ATN = 0$	<1 ng/m³ @	$<1 \text{ ng/m}^3 @ ATN =$
(1s timebase,	$50 \text{ ng/m}^3 \otimes  ATN  =$	ATN = 0	0
3.8 LPM)	30	50 ng/m³ @	50 ng/m³ @
		ATN  = 30	ATN  = 30
Sensitivity / Limit of	700 ng/m³ @ 3.8	400 ng/m <sup>3</sup> @ 3.8	260 ng/m <sup>3</sup> @3.8
detection	LPM, 1s	LPM, 1s	LPM, 1 s
(mean + 2σ)	40 ng/m³ @3.8 LPM,	25 ng/m³ @3.8	15 ng/m <sup>3</sup> @3.8
	1 min	LPM, 1 min	LPM, 1 min
Precision	<10%	<10%	<10%
Measurement	BC: 27%	BC: 27%	BC: 27%
uncertainty	Source	Source	Source
	apportionment: 30%	apportionment: 30%	apportionment: 30%
Measuring range (measuring interval, working interval)	0 – 100 μg/m³	0 – 100 μg/m³	0 – 100 μg/m³

gerosolmageesci.com Page 22 of 31

## 9. New GUI design

The new GUI can be navigated by pressing the icons in the vertical menu bar on the left side of the screen. The settings are divided into eight groups (Home, General, Data, QA/QC, External device and protocols, Settings, System and Info). Easy to use, the redesigned layout includes helpful additions, including a graphical data display on the "Data/Graph" screen and a wind regression analysis on the "Data/Pollution rose" panel (Figure 13). The graphical data display can plot a time series of compensated absorption coefficient values, or BC concentration, in real-time or for the selected period. The Pollution rose can be used to identify the air pollution source location. Note that the wind sensor must be connected to an external device for this analysis.

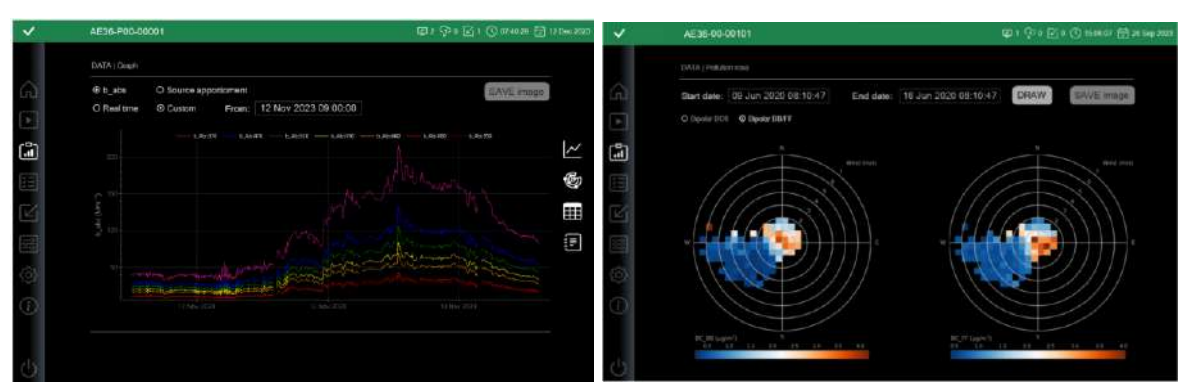


Figure 13. Graphical data presentation on AE36s- time-series of absorption coefficient at 7 wavelengths (left), and Pollution rose (right).

gerosolmageesci.com Page 23 of 31

## 10. Data Auto validation and new STATUS logics

Validating data is a crucial component of quality control and assurance (QA/QC). The new status control allows for a quick overview of the Instrument's status and easy filtering of valid data.

The Instrument's General Status is indicated by The color of the top line of the screen, the status description on the "Home" screen, and the LED indicator next to the screen. The colors indicate:

- Green = Instrument is measuring without warning.
- Green and blinking = The Instrument is running in QA/QC mode with no warnings, or the Instrument is conducting tape advance.
- Orange = Instrument is running with warnings; check status.
- Red = Instrument is stopped or in error.

Pressing the Status icon on the far left of the status line or the status indicator symbol on the home page will display the detailed status code and short sub-status description (Figure ).

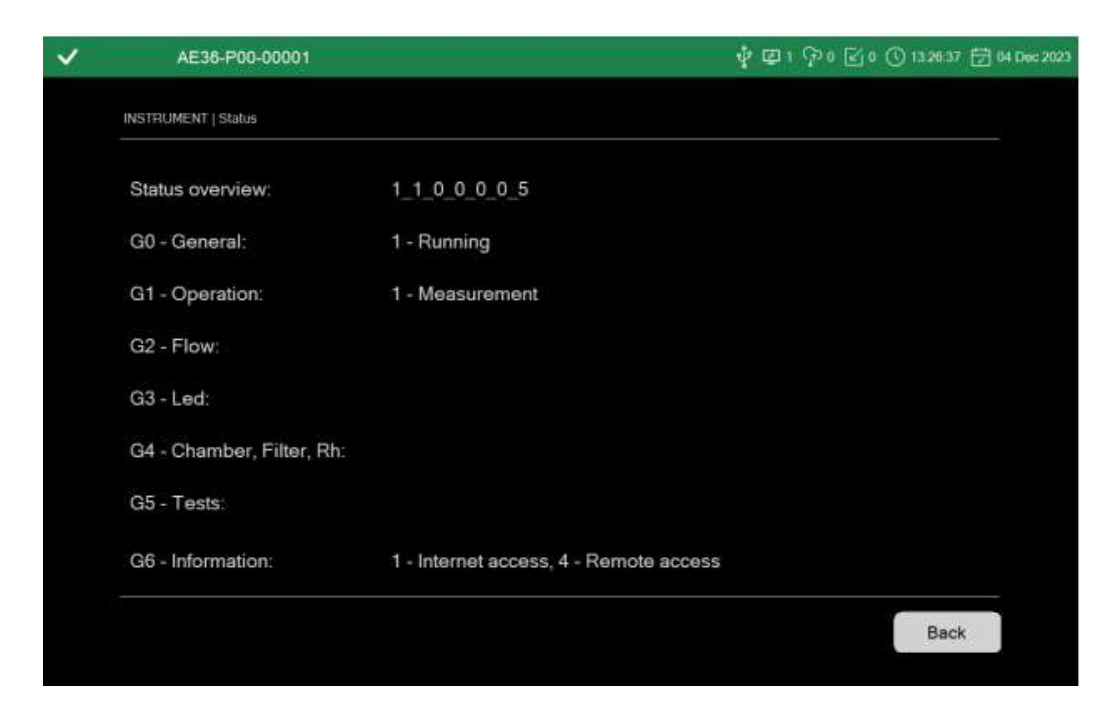


Figure 14. Instrument Status screen shows the Instrument's status overview and the deconvolution of the instrument status.

The status code of the Instrument consists of seven sub-status values, which are eightbit sets. The Instrument's general state is displayed in the first set, "G0".

The second set, "G1", will show the operation the Instrument is performing. "G2", "G3," and "G4" will show information on mechanical components, "G5" denotes QA/QC tests, and "G6" Information on connectivity, storage, etc.

With this status code, the data can be processed more quickly by filtering out only valid measurement data – data lines with the Status code G1=1, thus excluding data lines with

#### AEROSOL MAGEE SCIENTIFIC

errors, warnings, calibration values, and QA/QC tests. This filter can be applied on the Export Data screen, where users can download measurement data using the "validated" option.

gerosolmageesci.com Page 25 of 31

## 11. Optimized maintenance

An extended period of unsupervised operation was envisioned for AE36s. Several safety and diagnostic features ensure the Instrument is running optimally while having complete control over the Instrument and data quality.

The AE36s can operate unattended for extended periods thanks to their robust construction, automatic zero testing, and smooth connectivity wherever you are, thanks to the RAS module in the new CAAT software. Thus reducing the site visits and the operator's workload.

The Self-cleaning procedure was also developed to clean the optical chamber and internal tubing. This procedure uses valves and pumps to create alternating high and low pressure in the system, which removes the dirt deposited with time. The dirt is collected on the filter tape. After the procedure, a clean air test is recommended to ensure that the analytical area is free of particles or dirt. The <u>Self-cleaning procedure</u> reduces the buildup of dirt and other contaminants that may affect the data quality, significantly reducing maintenance and ensuring accurate readings over an extended period.

gerosolmageesci.com Page 26 of 31

## 12. Automatic Zero and Span

#### Zero

The AE36s Aethalometer can automatically check the 'zero-air' response of the Instrument under dynamic operating conditions. This test is implemented by backflushing the inlet connection with an excess flow of internally filtered air and circulating the filtered air in the Instrument.

The result of the clean air test is presented for all wavelengths and both spots in terms of:

- average BC concentration (AverageBC),
- point-to-point variation of BC concentration (PPBC),

The test result is acceptable if the values of

**PPBC** = 
$$\frac{1}{n} \sum_{i=0}^{n} |BC_{t_{i+1}} - BC_{t_i}|$$

are below the limits presented in the table below:

Wavelength	PPBC Spot 1	PPBC Spot 2
(nm)	(ng/m³)	(ng/m³)
370	220	750
470	180	590
520	200	660
590	220	740
630	230	790
880	330	1100
950	360	1200

If one of the reported values of PPBC on Spot 1 is larger than this limit value, inspect and clean the optical chamber. The average BC values should be close to zero if the Aethalometer is warmed up and stabilized for at least one hour. A short transient may be initially seen due to a filter compression artifact.

aerosolmageesci.com

#### Span

The AE36s Aethalometer's optical detectors' response may be verified using a kit of Neutral Density optical filters, as shown in Figure 16 below. These are glass elements with a range of known and stable optical absorptions, from light to dark, which are traceable from manufacturing records to primary standards. When inserted into the AE36 Aethalometer, the photodetectors give a certain output signal. The stability and reproducibility of the relationship between the optical signal and ND Filter density from one validation test to another, and the comparison with the original factory values, is a measure of the consistency of performance of the Instrument's optics.



Figure 16. The Optical Validation Kit consists of traceable standard Neutral Density Optical Filters inserted into the AE36s optical path to determine the reproducibility of the relationship between LED optical source intensity and detector response.

gerosolmageesci.com Page 28 of 31

## 13. Remote Access System (RAS)

The RAS application (Figure 17) is a software tool running on Windows (7, 10, or 11) operating system for remote control and downloading of the AE36 and AE36s Aethalometers' data remotely.

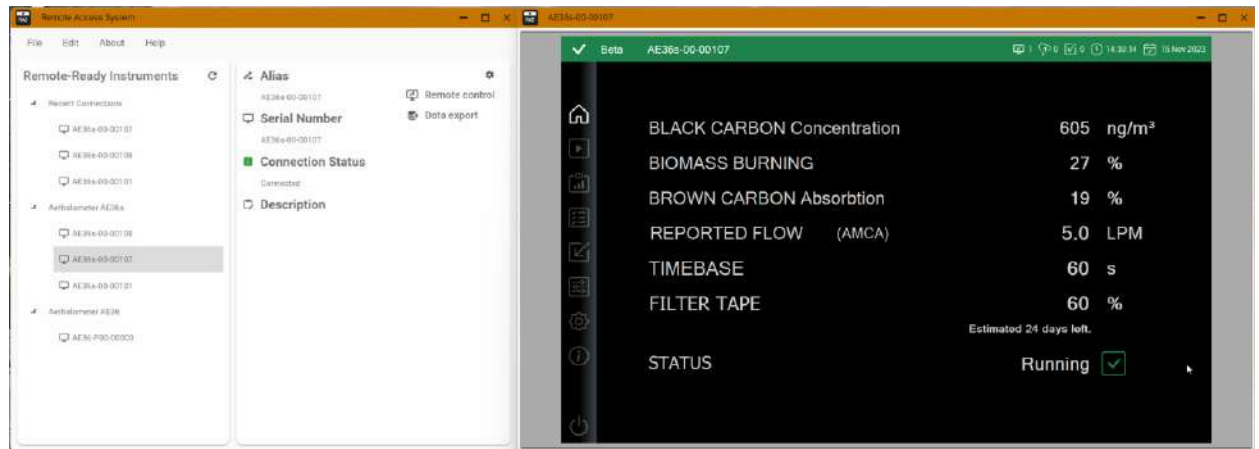


Figure 1. The left window shows a list of remote-ready instruments in the Remote Access System window, and on the right, the Instrument remote window displays the selected Instrument's Home screen.

RAS allows the user to remotely control and download data from any AE36/AE36s instrument connected to the same network as the computer they are currently remotely connecting to or from any instrument within that subnet available for remote connection.

Following the setup of the connection, an additional instrument window will appear next to the instrument remote window on the RAS Main Home screen. On this screen, operators can navigate, investigate, and alter the Instrument's operation as if the actual Instrument's graphical user interface were in front of them.

gerosolmageesci.com Page 29 of 31

#### 14. User and Communications Interfaces

The AE36s Aethalometer incorporates the following user, data, and communications features:

- Large color graphics touch-screen for data display and local user interface;
- USB ports for insertion of a memory stick for local data download;
- USB ports for connection of a keyboard, if necessary, for initial setup of parameters, such as station identification;
- RS-232 COM port for data transmission to digital datalogger;
- Ethernet port for full network access and control, including
  - i. Remote data acquisition, either batch or streaming
  - ii. Remote retrieval of instrument status and state-of-health
  - iii. Remote control of instrument operating parameters

#### 15. Modular Construction

The AE36s Aethalometer is constructed with a modular design so sub-units can be easily serviced. The only item requiring attention in routine use is cleaning the optical insert to remove accumulated dust or other contamination that may be brought in with the sample air stream. The optical chamber is attached with a bayonet fitting for quick removal; easy cleaning; and reliable re-assembly. The entire Instrument is hermetically sealed to reduce the entry of dust and moisture.

gerosolmageesci.com Page 30 of 31

## 16. Contact

Aerosol d.o.o. Kamniška 39 A SI-1000 Ljubljana Slovenia, EU

tel: +386 1 4391 700

https://www.aerosolmageesci.com/

AEROSOL MAGEE SCIENTIFIC

or the distributor responsible for your country.

Ljubljana, February 2024

aerosolmageesci.com Page 31 of 31